BJR

Received:
30 October 2014

Revised:
23 January 2015

Accepted:
3 February 2015

doi: 10.1259/bjr.20140721

Cite this article as:
Çavusoglu M, Duran S, Hatipoglu HG, Cılız DS, Elverici E, Sakman B. Petrous apex cephalocoele: contribution of coexisting intracranial pathologies to the aetiopathogenesis. Br J Radiol 2015;88:20140721.

FULL PAPER

Petrous apex cephalocoele: contribution of coexisting intracranial pathologies to the aetiopathogenesis

M ÇAVUSOGLU, S DURAN, H G HATIPOGLU, D S CILIZ, E ELVERICI and B SAKMAN

Department of Radiology, Ankara Numune Education and Research Hospital, Ankara, Turkey

Address correspondence to: Dr Mehtap Çavusoglu
E-mail: *mehtapcavusoglu2@gmail.com*

Objective: The aim of this study was to show the MRI findings of petrous apex cephalocoele (PAC) and the other intracranial pathologies that coexist with PAC, and to discuss the contribution of the co-existing pathologies to aetiopathogenesis.
Methods: A retrospective analysis of our imaging archive for the period from January 2012 to October 2013 revealed 13 patients with PAC (12 females and 1 male; age range, 26–69 years). 11 patients underwent MRI examination of the cranium, and 2 patients underwent MRI examination of the sellar region. We evaluated the lesions for content, signal intensity, enhancement, relation to petrous apex and Meckel's cave. Images were also evaluated for coexisting pathologies.
Results: The presenting symptoms included headache, vertigo, cerebrospinal fluid (CSF) leak and trigeminal neuropathy. All patients had PAC. All lesions were located posterolateral to the Meckel's cave and were isointense with CSF signal on all pulse sequences. All lesions were continuous with Meckel's cave. Coexisting pathologies included intracranial aneurysmal dilatation, empty sella, mass in hypophysis, arachnoid cyst, inferior herniation of parahippocampal gyrus and optic nerve sheath CSF distension.
Conclusion: Coexistence with other intracranial pathologies supports the possibility of CSF imbalance and/or intracranial hypertension in the aetiopathogenesis of PAC.
Advances in knowledge: This study examined the contribution of the co-existing intracranial pathologies to the aetiopathogenesis of PAC.

Petrous apex cephalocoele (PAC) is a rare cystic lesion of the petrous apex. It is characterized by herniation of the posterolateral wall of Meckel's cave into the petrous apex. It is also referred to as arachnoid cyst or meningocele. The aetiopathogenesis has not yet been clearly explained. It may be congenital or acquired. PAC may be detected incidentally in asymptomatic patients and does not necessitate treatment. However, it may lead to trigeminal neuropathy or leakage of cerebrospinal fluid (CSF) in some patients and may necessitate surgical treatment.[1,2]

Mucocele, trapped fluid, cholesterol granuloma, cholesteatoma, trigeminal cystic schwannoma and petrous apicitis may be considered in the differential diagnosis of petrous apex lesions.[3,4]

The coexistence of PAC and empty sella or arachnoid cyst has been reported in the literature and was suggested to support the possible role of disturbance of CSF circulation in pathophysiology.[2,5] In this study, we report the largest series of patients with PAC and other coexistent intracranial pathologies.

The aim of this study was to show the MRI findings of patients with PAC and coexistent intracranial pathologies, and to discuss the contribution of the coexisting pathologies to the aetiopathogenesis of PAC.

METHODS AND MATERIALS

This was a retrospective study, and a waiver was obtained from our institutional review board. A retrospective analysis of our imaging archives in the period extending from January 2012 to October 2013 revealed 13 patients with PAC (12 females and 1 male; age range, 26–69 years). All patients had undergone MRI examination (11 patients had undergone MRI examination of the cranium and 2 patients had undergone MRI examination of the sellar region). The images had been obtained using two distinct instruments, namely the 1.5-T Excite (GE Healthcare, Milwaukee, WI) and the 1.5-T Optima 450 W (GE Healthcare). For the cranial MRI, spin echo T_1 weighted images [repetition time (TR), 500 ms; echo time (TE), 9.6 ms; slice thickness, 5 mm; interslice gap, 1.5 mm; field of view (FOV), 24 × 18 cm; matrix, 320 × 192; number of excitations (NEX), two], fast-recovery fast spin echo T_2 weighted images (TR, 4,240 ms; TE, 98.1 ms; slice thickness, 5 mm; interslice gap, 1.5 mm; FOV, 24 × 18 cm; matrix, 352 × 224; NEX, two) and fluid-attenuated inversion recovery

(FLAIR) images (TR, 8,402 ms; TE, 95.5 ms; slice thickness, 5 mm; interslice gap, 1.5 mm; matrix, 288 × 192) were obtained. Diffusion-weighted sequence (TR, 10,000 ms; TE, 85.8 ms; slice thickness, 4 mm; interslice gap, 1 mm; matrix, 128 × 128) were performed with echo planar single-shot spin echo imaging with *b*-values of 0 and 1000 s mm^{-2}. Diffusion gradients were applied in three orthogonal directions to generate three sets of diffusion-weighted imagings (*x*, *y* and *z* axes). Apparent diffusion coefficient (ADC) values were automatically calculated. For MRI of the hypophysis, pre-contrast and post-contrast spin echo T_1 weighted sequences (TR, 675,00 ms; TE, 10.30 ms; slice thickness, 3 mm; FOV, 16 × 16 cm; matrix, 320 × 224; NEX, three), spin echo T_2 weighted sequences (TR, 3000 ms; TE, 87.24 ms; slice thickness, 3 mm; FOV, 16 × 16 cm; matrix, 320 × 224; NEX, three) were obtained in the sagittal and the coronal plains. Three-dimensional fast imaging employing steady-state acquisition (3D-FIESTA; TR, 4,8 ms; TE, 1.4 ms; slice thickness, 0.5 mm; FOV, 18 × 18 cm; matrix, 352 × 192; NEX, four) sequences were additionally obtained in three patients. The axial T_2 weighted fast-recovery fast spin echo sequence was used to measure optic nerve sheath diameter (ONSD). The axial image slice that provided the best view of the ONSD was chosen. The ONSD was measured in an axis perpendicular to the optic nerve, 3 mm behind the globe.[6] The images were evaluated by two experienced radiologists. Agreement between the two radiologists was reached in consensus after careful individual evaluation. The lesions were evaluated for content, signal intensity, relation to Meckel's cave and petrous apex. Images were also evaluated for the coexisting intracranial pathologies.

RESULTS

Ten patients presented with headache, one with vertigo, one with rhinorrhoea and one with trigeminal neuropathy. The patient with rhinorrhoea had a history of two duroplasties and meningitis in the past.

Eight patients had bilateral PAC, two had right PAC and three had left PAC. All lesions were located in the posterolateral portion of Meckel's cave. On MRI, all lesions were isointense to CSF signal intensity on all pulse sequences (low signal intensity on T_1 weighted and FLAIR images, and high signal intensity on T_2 weighted images). All lesions were continuous with Meckel's cave. In 11 patients, there was no diffusion restriction on diffusion-weighted images and the ADC map. We did not obtain diffusion-weighted imaging in two patients who had undergone pituitary MRI.

Eight patients had coexisting empty sella (Figure 1a–g). There were aneurysmal dilatations in the cavernous segment of the right internal carotid artery and the middle cerebral artery

Figure 1. A 38-year-old female presented with headache. Axial T_1 weighted (a), axial T_2 weighted (b), coronal T_2 weighted (c) and axial fluid-attenuated inversion recovery (d) MR images show bilateral petrous apex cephalocoele with cerebrospinal fluid content continuous with the Meckel's cave (arrows). Diffusion restriction is not noted on a diffusion-weighted image (e). Sagittal T_1 weighted MR image shows coexistent empty sella (f). Axial T_2 weighted MR image shows coexistent bilateral optic nerve sheath diameter distention (g).

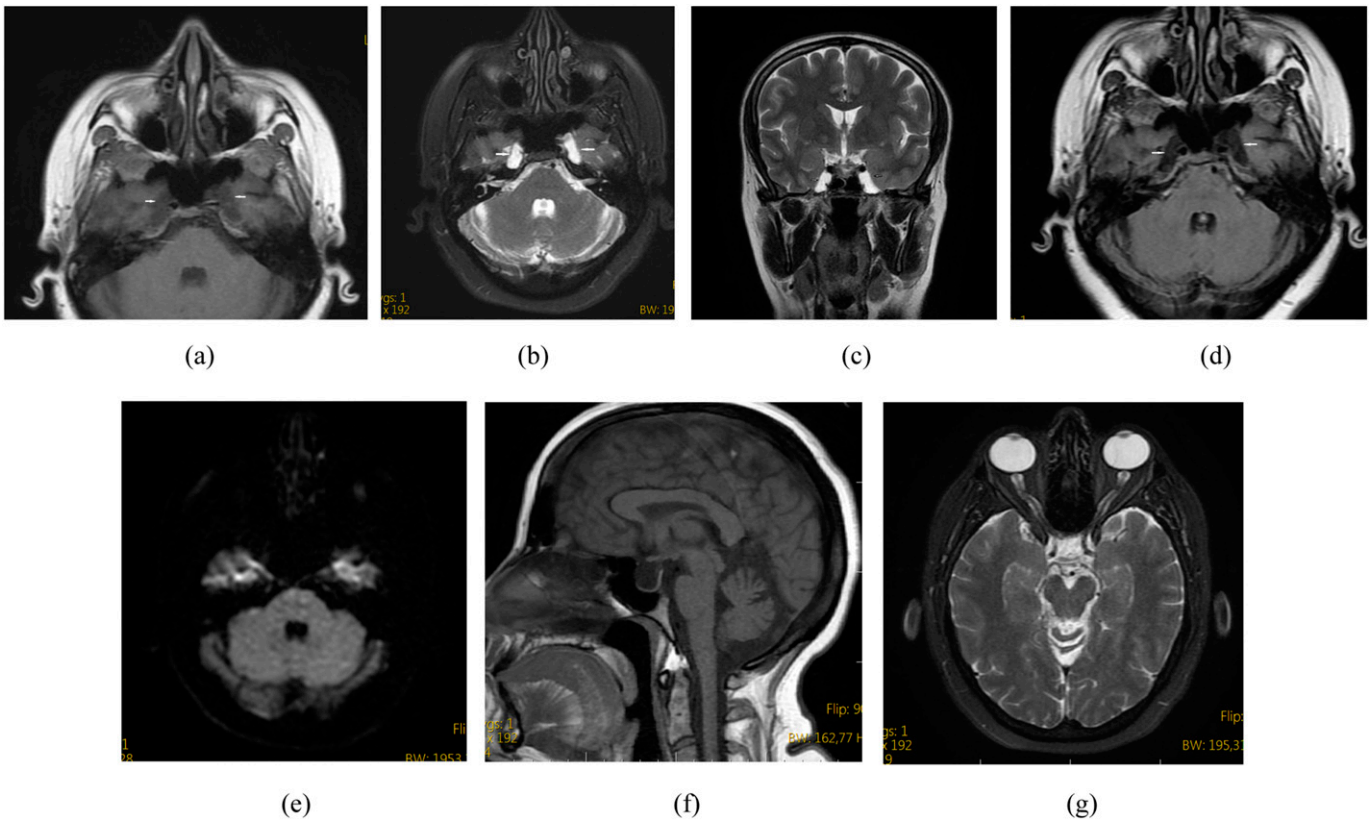

bifurcation, which were ipsilateral to PAC in one patient (Figure 2a–d). A left frontotemporal arachnoid cyst coexisting with PAC was observed in one patient (Figure 3a–e). In another patient, inferior herniation of the parahippocampal gyrus was observed on the left and also its indentation into the anterior aspect of the cysternal segment of the trigeminal nerve was seen (Figure 4a,b). A mass was detected in the hypophysis gland, coexisting with bilateral PAC in one patient. The patient had undergone a surgical intervention, and its pathology had been reported as granulomatous hypophysitis (Figure 5a–d). Optic nerve sheath distension and flattening of the posterior globes was observed in three patients as accompanying findings (Figure 1a–g).

DISCUSSION

PAC is a rare lesion of the petrous apex.[1] Cholesterol granuloma, cholesteatoma, apical petrositis, effusion or PAC should be considered in the differential diagnosis when a cystic mass is detected in the petrous apex.[2,7] PAC is characterized by herniation of the posterolateral wall of Meckel's cave into the petrous apex. None of the lesions mentioned in the differential diagnosis derive from Meckel's cave, except for PAC. Inflammatory lesions are derived within the petrous apex and may cause expansion. PAC, on the other hand, is derived from Meckel's cave and is extended into the petrous apex in a secondary manner.[1,2,8] The FLAIR and diffusion-weighted imaging sequences used in MRI play an important role in characterization of petrous apex lesions.[2] Cholesterol granulomas show hyperintensity in T_1 weighted and T_2 weighted sequences. The signal intensity of mucoceles is the same as that of effusions; however, mucoceles may demonstrate peripheral contrast uptake following administration of the contrast agent.[9–13]

Moore et al[1] have reported the largest series of ten patients with PAC. Eight of the ten patients were female. Three patients underwent surgery because of trigeminal neuropathy or otorrhoea. The surgical diagnosis was meningocele in two patients and arachnoid cyst in one patient. In the non-operative group, one patient had trigeminal neuralgia and the remaining patients were asymptomatic.

Alorainy[2] reported a group of five patients with PAC (four females and one male; age range, 25–60 years). The presenting

Figure 2. A 66-year-old female presented with headache. Coronal T_2 weighted MR image showing petrous apex cephalocoele (double arrow) on the right side (a). Axial T_2 weighted (b), sagittal T_1 weighted MR images (c) and digital subtraction angiography (d) demonstrate aneurysmal dilatation of the right internal carotid artery (arrow).

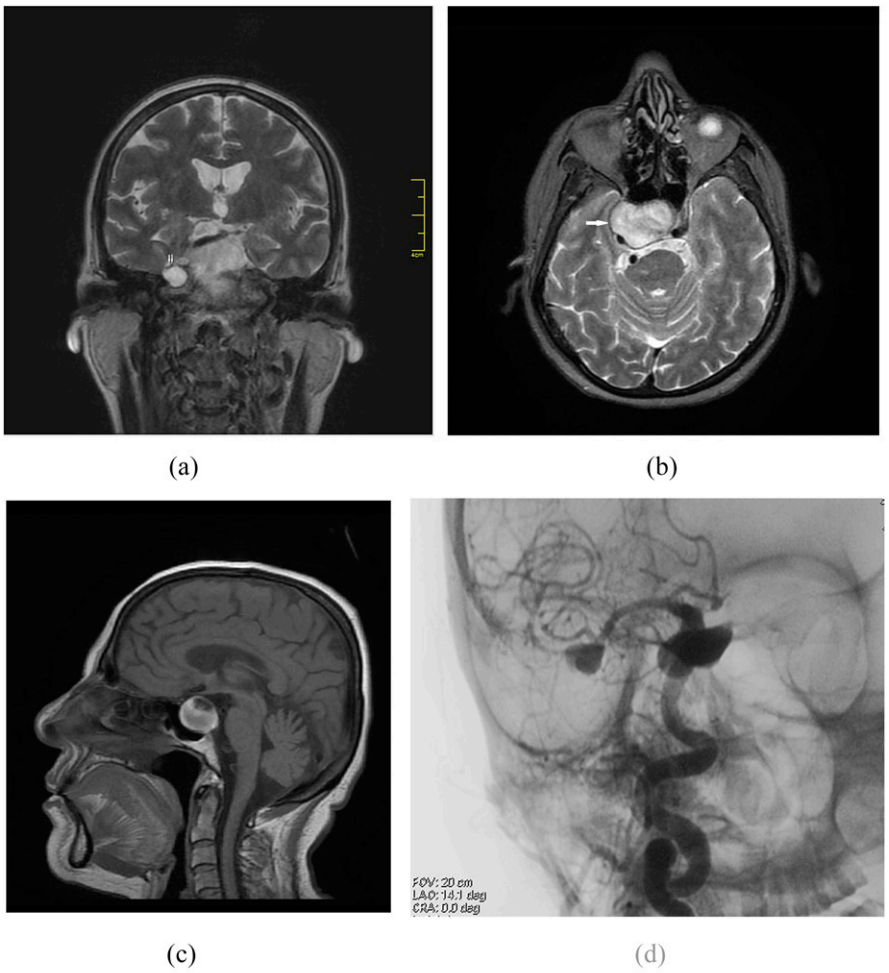

Figure 3. A 26-year-old male complaining of headaches. Coronal T_2 weighted (a) and axial T_2 weighted (b) MR images show bilateral petrous apex cephalocoele. Coronal (a), axial T_2 weighted (c), axial fluid-attenuated inversion recovery (d) and diffusion-weighted (e) MR images show coexistent arachnoid cyst (arrows) on the left side.

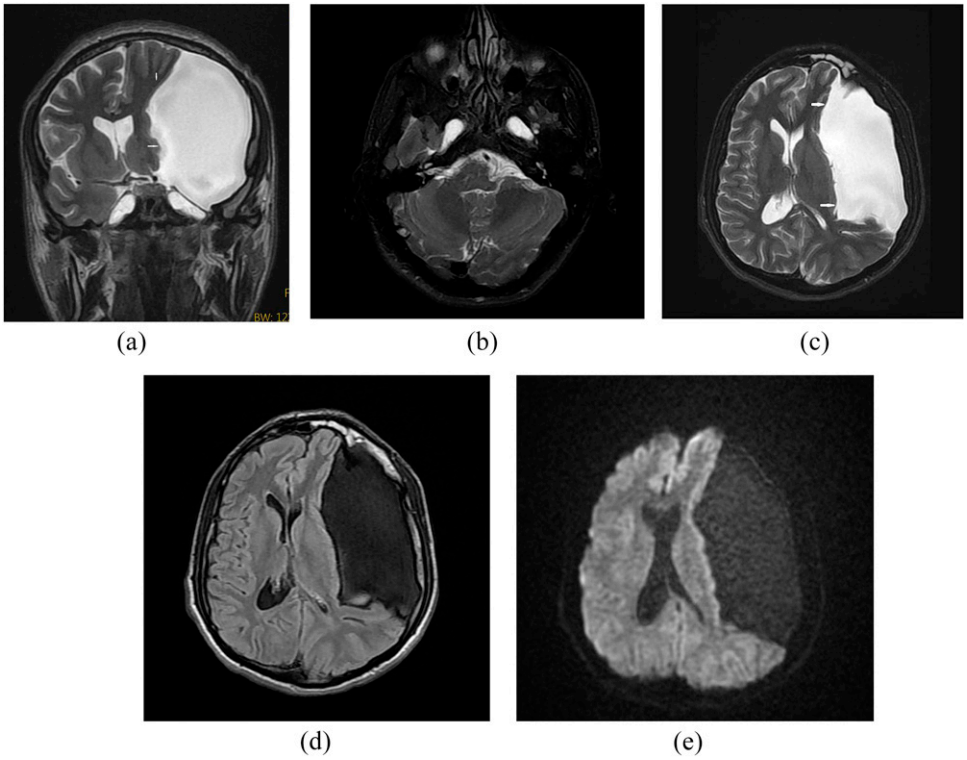

symptoms in all patients were not attributable to PAC (three patients presented with tinnitus and two patients presented with headaches). Four patients had bilateral PAC and one had left PAC. All patients had coexisting empty sella, and one patient had small arachnoid cyst in the middle cranial fossa.

Hatipoğlu et al[5] reported a group of four patients with PAC (four females; age range, 41–60 years). All patients were asymptomatic (three patients presented with headache and one patient presented with diplopia). All patients had bilateral PAC. Three patients had coexisting empty sella, and one patient had arachnoid cyst in the Sylvian fissure.

8 (61.5%) of the 13 patients with PAC in our group had coexisting empty sella. Many studies in the literature have reported the development of primary empty sella as a result of impaired CSF absorption. It has been reported that as a result of impaired CSF absorption, intracranial pressure (ICP) is increased; CSF and the meninges are herniated into the missing diaphragma sella; and an empty sella develops.[13–15]

Figure 4. A 30-year-old female presented with trigeminal neuralgia. Axial T_2 weighted (a) and coronal T_2 weighted (b) MR images show bilateral petrous apex cephalocoele (double arrow) and inferior herniation of parahippocampal gyrus on the left side (arrow).

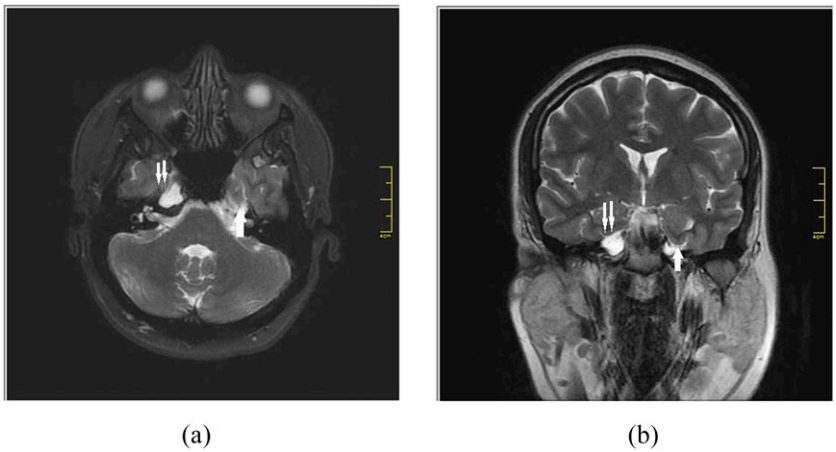

Figure 5. A 48-year-old female presented with irregular menstrual cycles. Coronal T_2 weighted (a) and axial T_2 weighted (b) MR images show bilateral petrous apex cephalocoele (arrows). Sagittal T_1 weighted pre-contrast (c) MR image shows pituitary expansion (arrow) and focal hypointense area inside of the gland (asterisk). Sagittal T_1 weighted post-contrast (d) MR image shows non-enhancing cystic lesion (asterisk) in homogeneously enhancing pituitary gland (arrow).

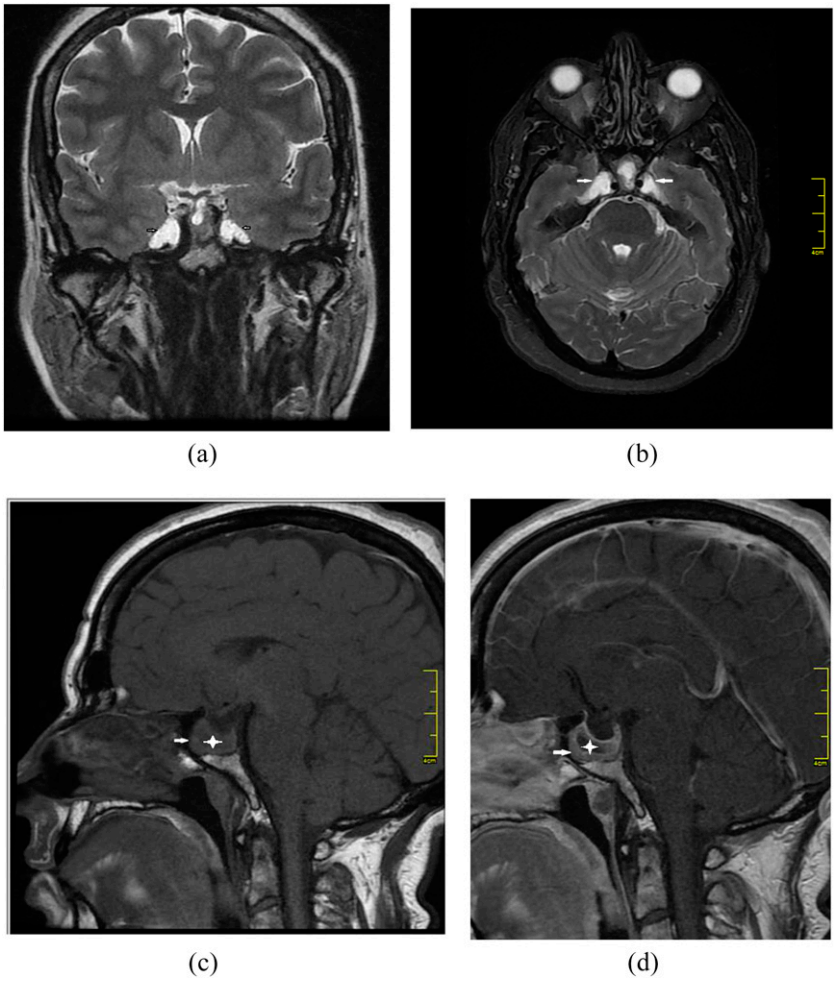

Many investigators have reported a strong relationship between empty sella and spontaneous CSF leakage. Female predominance is apparent in these groups. Schlosser and Bolger[14] have reported empty sella in all 15 patients with spontaneous rhinorrhoea and in 1 of 9 patients with non-spontaneous rhinorrhoea. Shetty et al[13] detected empty sella in 7 of 11 patients with spontaneous rhinorrhoea. Prichard et al[15] found empty sella in five of seven patients treated owing to CSF otorrhoea.

CSF leakage in the form of otorrhoea or rhinorrhoea has been reported in 7 of 22 patients with PAC in the literature. All of these patients were children between 4 and 13 years of age (three males, four females). The reasons for admission were recurrent meningitis, postural headache and transmission-type hearing loss.[1,8,16–18] Only one of the patients in the paediatric group had no CSF leakage.[9] Although other theories have also been suggested, spontaneous CSF leakage is believed to arise from defects in the skull base as a result of the increase in ICP.[13–15]

1 of the 13 patients with PAC in our group had a coexisting left frontotemporal arachnoid cyst. Arachnoid cysts are developmental cavities that are located within the arachnoid membrane. They are surrounded by collagen and arachnoid matter cells.[9] It has been reported that pulsatile CSF pressure may cause protrusion of the arachnoid granulomas from the weak points of the underlying dura layer and may have an effect in the formation of arachnoid cysts.[7] Alorainy[2] had detected empty sella in all five patients with PAC and arachnoid cyst in the middle cranial fossa in one patient. Hatipoğlu et al[5] have reported empty sella in all four patients with PAC and arachnoid cyst in the Sylvian fissure in one patient.

1 of the 13 patients with PAC in our group was male and 12 were female (age range, 26–69 years). Bilateral and unilateral PACs were detected in eight and five of the patients, respectively. All of the lesions were isointense with CSF in all sequences and demonstrated continuation with Meckel's cave. The reasons for presentation to the hospital were rhinorrhoea in one patient, trigeminal neuralgia in one, and headache and vertigo in the remaining patients. PAC was accompanied by empty sella in 7 of the 13 patients. Three of these patients were determined to have bilateral PAC and four were found to have unilateral PAC. In one patient, bilateral PAC was accompanied by a left

frontotemporal arachnoid cyst. These findings support the studies of Alorainy[2] and Hatipoğlu et al.[5]

One of our patients (a 45-year-old female patient) had rhinorrhoea. Coexistence of PAC and rhinorrhoea has only been reported in paediatric patients in the literature.[1,16–18] This is the first time that this coexistence is being reported in adult patients. The patient had bilateral PAC, and previous meningitis was present in her history. In the same patient, the findings were accompanied by bilateral optic nerve sheath CSF distention. No CSF leakage has been reported in adult patients with PAC in the literature.

Geeraerts et al[6] have demonstrated that distension of the ONSD is related to ICP. The optic nerve is surrounded by CSF, which shows continuity with intracranial CSF. When the ICP is increased, distension can be observed in the optic nerve sheath.[19–22] Fat-suppressed T_2 weighted sequence of the MRI can be used in the measurement of the ONSD.[23,24] If the ONSD turns out to be >5.82 mm, the probability of increased ICP is 90%.[18] In our study, optic nerve sheath distension was detected in 3 out of 13 patients (the ONSD was >5.82 mm in all 3 patients). There was also flattening of the posterior globes on imaging. All of the three patients were female, and also bilateral PAC was present in all of them. Empty sella coexisted in two of the three patients. Two of the patients were asymptomatic and one had rhinorrhoea.

Maira et al[25] performed continuous ICP monitoring on 11 patients with idiopathic empty sella syndrome. 27% of the patients had elevated ICP while awake, 45% had elevated ICP while in rapid eye movement sleep and only 27% had normal ICP at all times. The spectrum of intracranial hypertension probably begins with milder, intermittent forms and ends with more severe forms that develop benign intracranial hypertension or pseudotumour cerebri.[14] Although ICP was not measured in the reported cases of our study, this would explain why distention of ONSD was present only in 3 of the 13 patients with PAC in this study.

Schlosser and Bolger[14] and Prichard et al[15] determined a correlation between empty sella and spontaneous CSF rhinorrhoea and otorrhoea in their studies. The role of elevated ICP in spontaneous CSF otorrhoea/rhinorrhoea has also been reported.[14,15]

In this study, the coexistence of PAC and empty sella, arachnoid cyst, CSF leakage and optic nerve sheath distension have been presented. The female predominance is apparent in our study (92.3%). These findings demonstrate that impaired CSF absorption and an increase in ICP may play a role in the aetiopathogenesis of PAC.

To our knowledge, there is no previous report of coexistence of PAC with aneurysmal dilatation, hypophyseal mass or herniation of the parahippocampal gyrus. Considering that raised ICP is one of the major causes of PAC,[2,5] it would be possible to discuss its role if ICP was measured in the reported cases, which is a limitation of this study. To clarify the aetiopathogenesis of PAC, it seems important to measure ICP in future cases.

The differentiation between cholesteatoma and PAC should be made accurately in order to avoid unnecessary surgical interventions.[1,8,18] Cholesteatomas demonstrate high signal intensity, and PAC demonstrates low signal intensity in FLAIR sequences.[9,10] Cholesteatomas demonstrate diffusion restriction in diffusion-weighted images and are observed as hyperintense.[11] In this study, diffusion-weighted imaging was performed in 11 patients, and cholesteatoma was excluded from the differential diagnoses.

The 3D-FIESTA sequence was used in three patients in our study. The 3D-FIESTA sequence provides optimal imaging of the cranial nerves and the anatomical details of small vascular structures. High-resolution, high-quality images can be obtained, and the images can be easily reformatted in any plane with excellent quality.[26–28] With these properties, the 3D-FIESTA sequence has been quite effective in demonstrating the relationship between the extensions of PAC and the neighbouring structures and in the imaging of the trigeminal nerve.

CONCLUSION

Although the number of patients in this report does not allow for statistical inferences or definite conclusions, the coexistence of PAC with arachnoid cyst, empty sella, distension of ONSD or otorrhoea/rhinorrhoea supports the possibility of CSF imbalance and/or intracranial hypertension in the aetiopathogenesis.

REFERENCES

1. Moore KR, Fischbein NJ, Harnsberger HR, Shelton C, Glastonbury CM, White DK, et al. Petrous apex cephaloceles. *AJNR Am J Neuroradiol* 2001; **22**: 1867–71.
2. Alorainy IA. Petrous apex cephalocele and empty sella: is there any relation? *Eur J Radiol* 2007; **62**: 378–84.
3. Moore KR, Harnsberger HR, Shelton C, Davidson HC. "Leave me alone" lesions of the petrous apex. *AJNR Am J Neuroradiol* 1998; **19**: 733–8.
4. Connor SE, Leung R, Natas S. Imaging of the petrous apex: a pictorial review. *Br J Radiol* 2008; **81**: 427–35. doi: 10.1259/bjr/54160649
5. Hatipoğlu HG, Çetin MA, Gürses MA, Dağlıoğlu E, Sakman B, Yüksel E. Petrous apex cephalocele and empty sella/arachnoid cyst coexistence: a clue for cerebrospinal fluid pressure imbalance? *Diagn Interv Radiol* 2010; **16**: 7–9. doi: 10.4261/1305-3825.DIR.2650-09.2
6. Geeraerts T, Newcombe VF, Coles JP, Abate MG, Perkes IE, Hutchinson PJ, et al. Use of T2-weighted magnetic resonance imaging of the optic nerve sheath to detect raised intracranial pressure. *Crit Care* 2008; **12**: R114. doi: 10.1186/cc7006
7. Curtin HD, Chavali R. Imaging of the skull base. *Radiol Clin North Am* 1993; **36**: 801–17.
8. Motojima T, Fujii K, Ishiwada N, Takanashi J, Numata O, Uchino Y, et al. Recurrent meningitis associated with a petrous apex cephalocele. *J Child Neurol* 2005; **20**: 168–70.
9. Batra A, Tripathi RP, Singh AK, Tatke M. Petrous apex arachnoid cyst extending into

Meckel's cave. *Australas Radiol* 2002; **46**: 295–8.
10. Chang P, Fagan PA, Atlas MD, Roche J. Imaging destructive lesions of the petrous apex. *Laryngoscope* 1998; **108**: 599–604.
11. Alkilic-Genauzeau I, Boukobza M, Lot G, George B, Merland JJ. CT and MRI features of arachnoid cyst of the petrous apex: report of 3 cases. [In French.] *J Radiol* 2007; **88**: 1179–83.
12. Larson TL, Wong ML. Primary mucocele of petrous apex: MR appearance. *AJNR Am J Neuroradiol* 1992; **13**: 203–4.
13. Shetty PG, Shroff MM, Fatterpekar GM, Sahani DV, Kirtane MV. A retrospective analysis of spontaneous sphenoid sinus fistula: MR and CT findings. *AJNR Am J Neuroradiol* 2000; **21**: 337–42.
14. Schlosser RJ, Bolger WE. Significance of empty sella in cerebrospinal fluid leaks. *Otolaryngol Head Neck Surg* 2003; **128**: 32–8.
15. Prichard CN, Isaacson B, Oghalai JS, Coker NJ, Vrabec JT. Adult spontaneous CSF otorrhea: correlation with radiographic empty sella. *Otolaryngol Head Neck Surg* 2006; **134**: 767–71.
16. Mulcahy MM, McMenomey SO, Talbot JM, Delashaw JB Jr. Congenital encephalocele of the medial skull base. *Laryngoscope* 1997; **107**: 910–14.
17. Schick B, Draf W, Kahle G, Weber R, Wallenfang T. Occult malformations of the skull base. *Arch Otolaryngol Head Neck Surg* 1997; **123**: 77–80.
18. Cheung SW, Broberg TG, Jackler RK. Petrous apex arachnoid cyst: radiographic confusion with primary cholesteatoma. *Am J Otol* 1995; **16**: 690–4.
19. Hansen HC, Helmke K. The subarachnoid space surrounding the optic nerves. An ultrasound study of the optic nerve sheath. *Surg Radiol Anat* 1996; **18**: 323–8.
20. Helmke K, Hansen HC. Fundamentals of transorbital sonographic evaluation of optic nerve sheath expansion under intracranial hypertension. I. Experimental study. *Pediatr Radiol* 1996; **26**: 701–5.
21. Helmke K, Hansen HC. Fundamentals of transorbital sonographic evaluation of optic nerve sheath expansion under intracranial hypertension II. Patient study. *Pediatr Radiol* 1996; **26**: 706–10.
22. Hansen HC, Helmke K. Validation of the optic nerve sheath response to changing cerebrospinal fluid pressure: ultrasound findings during intrathecal infusion tests. *J Neurosurg* 1997; **87**: 34–40.
23. Mashima Y, Oshitari K, Imamura Y, Momoshima S, Shiga H, Oguchi Y. High-resolution magnetic resonance imaging of the intraorbital optic nerve and subarachnoid space in patients with papilledema and optic atrophy. *Arch Ophthalmol* 1996; **114**: 1197–203.
24. Lam BL, Glasier CM, Feuer WJ. Subarachnoid fluid of the optic nerve in normal adults. *Ophthalmology* 1997; **104**: 1629–33.
25. Maira G, Anile C, Cioni B, Menini E, Mancini A, De Marinis L, et al. Relationships between intracranial pressure and diurnal prolactin secretion in primary empty sella. *Neuroendocrinology* 184; **38**: 102–7.
26. Amemiya S, Aoki S, Ohtomo K. Cranial nerve assessment in cavernous sinus tumors with contrast-enhanced 3D fast-imaging employing steady-state acquisition MR imaging. *Neuroradiology* 2009; **51**: 467–70. doi: 10.1007/s00234-009-0513-z
27. Prieto R, Pascual JM, Yus M, Jorquera M. Trigeminal neuralgia: assessment of neurovascular decompression by 3D fast-imaging employing steady-state acquisition and 3D time of flight multiple overlapping thin slab acquisition magnetic resonance imaging. *Surg Neurol Int* 2012; **3**: 50. doi: 10.4103/2152-7806.96073
28. Hatipoğlu HG, Durakoğlugil T, Ciliz D, Yüksel E. Comparison of FSE T2W and 3D FIESTA sequences in the evaluation of posterior fossa cranial nerves with MR cisternography. *Diagn Interv Radiol* 2007; **13**: 56–60.